MEASUREMENT AND SIMULATION OF SUBSTANCE SPECIFIC CONTRIBUTIONS OF PHYTOPLANKTON, GELBSTOFF, AND MINERAL PARTICLES TO THE UNDERWATER LIGHT FIELD IN COASTAL WATERS

Hans Barth, Rainer Reuter & Marc Schröder

Carl von Ossietzky Universität Oldenburg
Fachbereich Physik, D-26111 Oldenburg, Germany

ABSTRACT

Hydrographic conditions in coastal waters are often characterized by large amounts of dissolved and particulate matter. These substances influence the optical water properties and the radiative transfer in the water column. Optical *in situ* instruments allow measurements of vertical distributions of absorbing, scattering, and fluorescent matter in the water column. A high vertical resolution is of interest to characterize the state and the dynamics of biological and chemical systems and to validate theoretical results from simulated computations. The role of such quantities as basic parameters for radiative transfer calculations is evident and presented here.

Algorithms for a specific evaluation of mineral particles, phytoplankton, and gelbstoff are developed for attenuation spectra. The calculated data set includes size distributions of mineral particles and phytoplankton, intracellular chlorophyll content and gelbstoff concentration. The wavelength-dependent scattering coefficients for mineral particles and phytoplankton are also determined. With this information phase functions are calculated and radiative transfer calculations are performed. The simulations of the underwater light field are compared with measurements.

INTRODUCTION

The measurement of fluorescent and absorbing matter in the water column is well known in marine biology and chemistry.[1,2]. Prominent examples of optically detectable substances are gelbstoff (yellow substance or Coloured Dissolved Organic Matter CDOM), mineral particles, and chlorophyll a as well as other phytoplankton pigments. In this paper, we report on a new method to calculate the submarine light field from known spectra of attenuation coefficients.
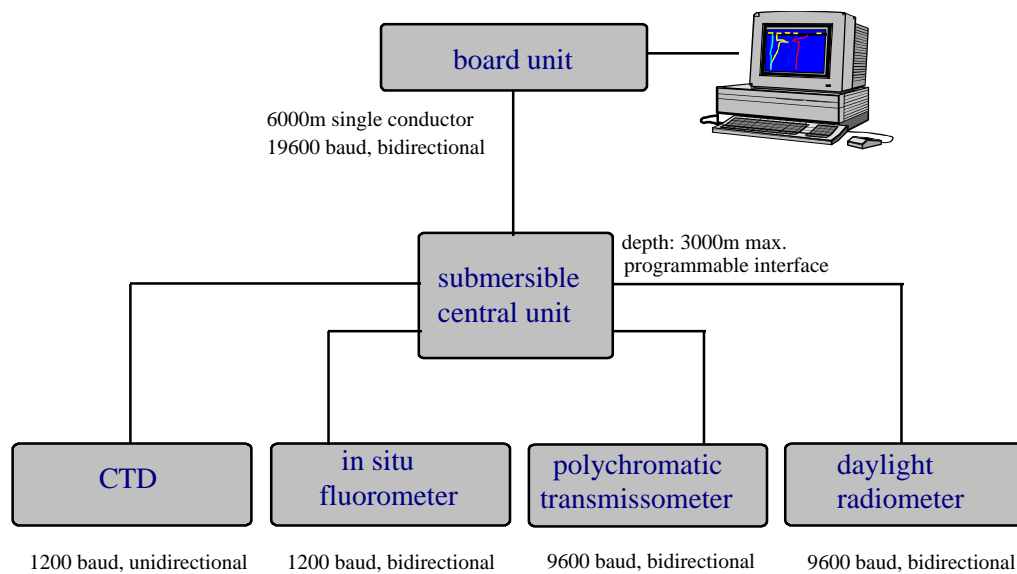
Figure 1: Schematic diagram of the bio-optical *in situ* probing system.

In the first part, a method is presented which allows the attenuation spectra to be interpreted in terms of the substances given above. Results obtained along a transect in the Seine Bight are shown. Fluorescence data and interpreted attenuation spectra are used to quantify the concentrations of gelbstoff and chlorophyll. Together with information on mineral particles, and CTD data, the substance distributions are discussed in terms of hydrographic conditions. In the second part, a radiative transfer code is used to simulate the light field at a station of the transect in the Seine Bight. With concentrations taken from transmissometer data interpretation the radiative transfer code is used to calculate profiles of scalar irradiance, which are in very good agreement with measured profiles.

INSTRUMENTS

Depth profiles were made with a bio-optical probing system,[3] Figure 1, consisting of:

1. a fluorometer, with excitation at 3 wavelengths that can be set in the UV and/or VIS. Fluorescence emission is detected with a modular set-up of up to ten detection channels at selectable wavelengths.[4]

2. a radiometer, equipped with a downward and an upward looking hemispherical $(E_O + \vec{E})/2$ collector.[5] The data are used to calculate the scalar irradiance E_O and the net (vector) irradiance $\vec{E}$ (1,2). The spectra are detected with two miniaturized CARL ZEISS spectrometers, each having 134 channels from 340 to 760 nm. The data that are transmitted via telemetry on board the ship consist of two times 43 channels at wavelengths that are selectable for an optimal data interpretation.

3. a transmissometer, that uses miniaturized CARL ZEISS spectrometers to measure spectra of the beam attenuation coefficient c at 375-755 nm. The instrument is equipped with a movable retroreflector to fit the path length in water to a broad range of turbidity and to achieve an *in situ* calibration. The data interpretation includes algorithms to classify scattering and absorbing matter in terms of phytoplankton, transparent particles, and gelbstoff.[6]

4. a CTD Model OTS 1500 (ME Meerestechnik-Elektronik, Germany) equipped with sensors for measuring pressure, conductivity, temperature, and oxygen. From the data, salinity and density are calculated according to UNESCO standards.[7]
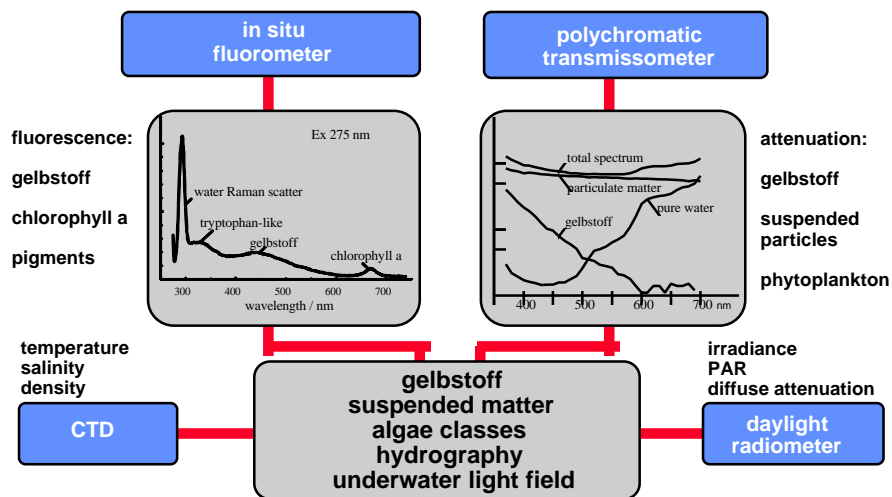
Figure 2: Parameters and substance-specific data that are derived with the bio-optical probing system.

Additional measurements were performed in the ship laboratory with a Perkin Elmer Lambda 18 spectrophotometer and a LS 50 spectrofluorometer. These data were used for the calibration and validation of *in situ* data. The *in situ* profiles for chlorophyll are calibrated to *chl a* concentrations

that were measured with High Pressure Liquid Chromatography (HPLC) by the GKSS Research Centre Geesthacht, Germany, and by the Laboratoire de Physique et Chimie Marines (LPCM), Villefranche-sur-Mer, France.

SUBSTANCE-SPECIFIC ATTENUATION SPECTRA

The *in situ* polychromatic transmissometer measures the intensity loss of a near-parallel light beam along *a* light path *r* in water, yielding data on the total attenuation coefficient *c*. The wavelength-dependent coefficient *c* of Lambert's law $dI/I = -cr$ is a composite of several terms, which describe absorption and scattering by molecules and particles:

$$c(l) = c_w(l) + c_{pp}(l) + c_{tp}(l) + a_d(l)$$

where the indices *w*, *pp*, *tp*, and *d* refer to contributions from water, phytoplankton, transparent (mineral) particles, and gelbstoff. When compared with instruments for single wavelength operation, the advantage of multispectral transmissometry lies in the information content of the entire attenuation spectrum, from which substance-specific features can be extracted. In a second step, these features can then be related to absolute quantities such as substance concentrations. This can be done with *chl a* and transparent particles, while gelbstoff is defined by the absorption coefficient of filtered water.

Within the accuracy of the instrument, the attenuation coefficient of water c_w is independent of temperature and salinity in the spectral range of 370 to 700 nm. Therefore, a spectrum of purified water, free of dissolved organic matter and particles due to active carbon and membrane filtration, is subtracted from the total spectrum $c(l)$ as a first step of data interpretation. With these assumptions, the attenuation coefficient can be written as:

$$c(l) - c_w(l) = a c_{pp}^*(l) + b c_{tp}^*(l) + g a_d^*(l)$$

where the terms with an asterisk are dimensionless spectral functions related to specific substances or substance classes as defined previously. The goal of the data interpretation is to determine the factors **a**, **b**, and **g**, which describe the relative contributions of individual substances to the entire spectrum. Moreover, certain parameters which determine the spectral functions $c_{pp}^*(?)$ and $c_{tp}^*(?)$ are determined.

The phytoplankton-specific spectrum $c_{tp}^*(?)$ is calculated using a Mie scattering algorithm with the following assumptions:
- particles are spherical
- the particle size distribution is monodisperse
- chlorophyll is homogeneously distributed in the phytoplankton cells
- the refractive index is described by the real and imaginary part $m(?) = n(?) + in´(?)$.

The specific spectrum of transparent particles $c_{tp}^*(?)$ is also calculated using a Mie scattering algorithm, where
- particles are spherical
- the particle size distribution $N(r)$ is hyperbolic, that is a Junge-type distribution $N(r) \propto r^{-c_j}$, with the Junge coefficient c_j ranging between 3 and 6.
- the refractive index is set constant and real, $m(?) = n(?)$, hence particles are free from absorption.

The absorption spectrum of gelbstoff is described by the empirical relation $a_d^*(?) = exp(-S?)$, with S=0.014/nm.[8]

The optimum parameter set minimizes the deviation of measured and reconstructed spectra (Figure 3) by searching for a minimum of the deviation function

$$D = \left| \{c(\boldsymbol{l}) - c_w(\boldsymbol{l})\} - \boldsymbol{a} c_{pp}^*(\boldsymbol{l}) - \boldsymbol{b} c_{tp}^*(\boldsymbol{l}) - \boldsymbol{g} a_d^*(\boldsymbol{l}) \right|.$$

This is done with the Levenberg-Marquard least square algorithm[8] in MATLAB® for a real-time interpretation at high data rates, yielding information on chlorophyll, mineral particles, and the parameters of their Junge size distribution, and gelbstoff.
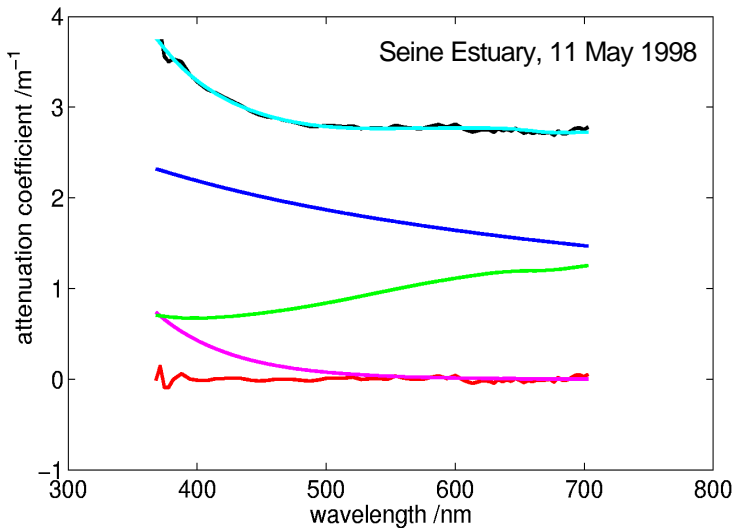
Figure 3: Example of a spectrum of the attenuation coefficient measured *in situ* in the Seine Estuary, see following section. Experimental data $c(\boldsymbol{l})$ (with the pure water spectrum $c_w(\boldsymbol{l})$ subtracted) are given as black line, partly hidden by the curve in light blue colour showing the reconstructed attenuation spectrum. This spectrum is the sum of specific compounds from gelbstoff (pink), phytoplankton (green), and mineral particles (dark blue). The red curve is the difference of the measured and reconstructed spectrum.

MEASUREMENTS IN THE SEINE BIGHT

Within the frame of the European project COAST*ℓ*OOC several field measurements were carried out in the outflows of the rivers Loire, Seine, Thames, Rhine, Elbe, Oder, and Rhone. Examples of the inherent optical properties, and of the temperature, salinity, and chlorophyll distribution in the Seine region are presented here. The location of the chosen transect in the outflow of the river Seine is shown in Figure 4. The transect started at station 15 at 49°22.4' N, 000°09.7' W and ended at station 22 at 49°45.0' N, 000°10.2' W. The mean distance between stations is 2.5 nautical miles.
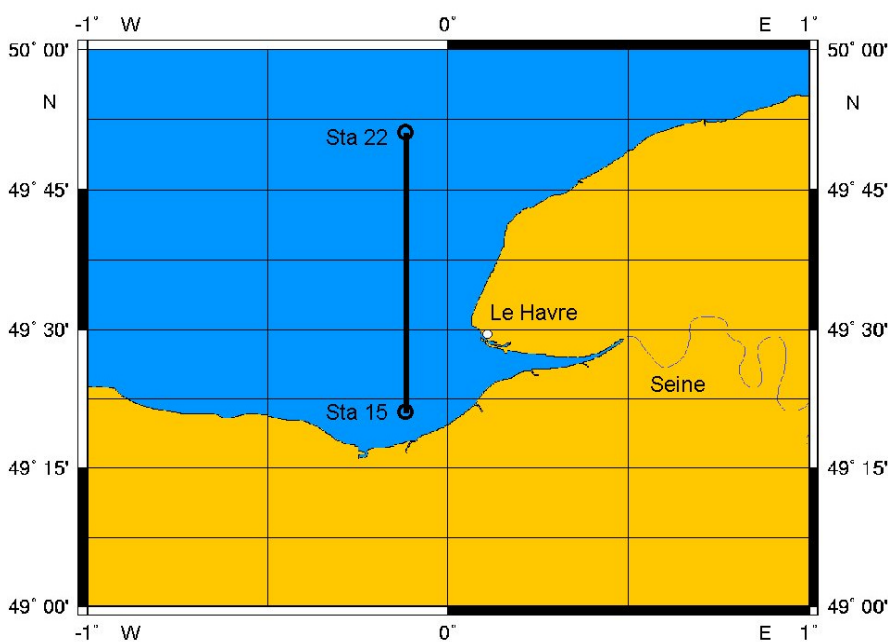
Figure 4: Location of the transect in the Seine Bight on 8 May 1998.

In Figures 5-6 data from *in situ* measurements of temperature and salinity are shown. The influence of the river Seine is dominant at stations 16 and 17 from the surface to depths of 5 to 10 m, with enhanced temperatures of 13 - 14 °C and low salinity of 28 - 29. At greater depths, and at stations 18 to 22 this influence vanishes gradually.
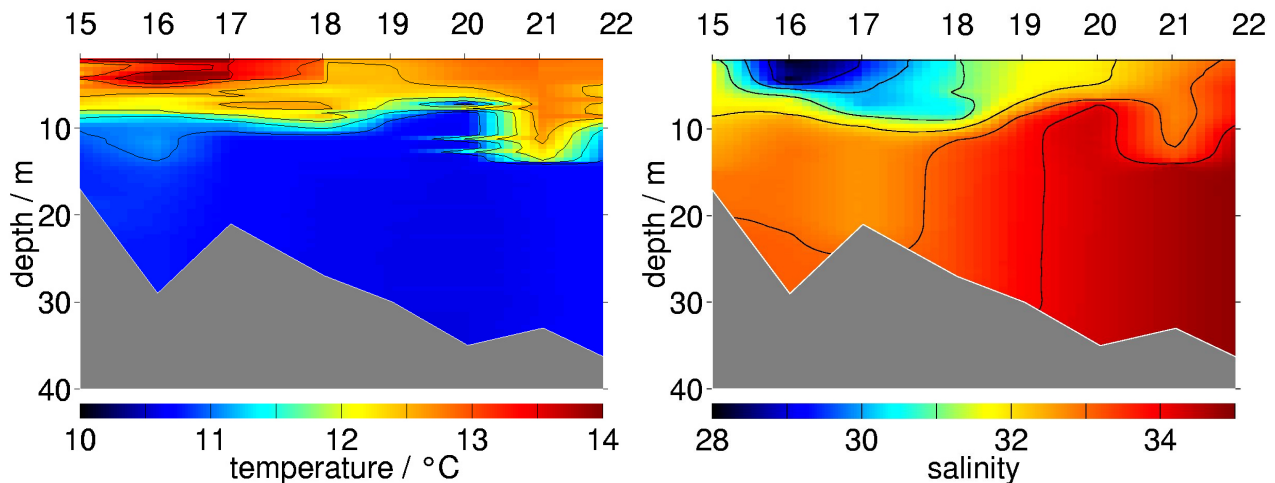
Figures 5 and 6: Temperature and salinity distribution along the transect in the Seine Bight on 8 May 1998.

Substance-specific data derived from spectra of the attenuation coefficient c are shown in Figures 7-9. The scattering coefficient of mineral particles depends on the wavelength and is shown for 400 nm wavelength in Figure 7. Strong scattering is measured near the mouth of the river, which is the main source of mineral particles in the Seine Bight. The absorption coefficient of gelbstoff is shown in Figure 8; it displays almost the same distribution as the salinity. The chlorophyll data, Figure 9, reveal highest concentrations of phytoplankton in the regions between the Seine river plume and the waters with higher salinity that originate from the English Channel.

The influence of the river water on mineral particle scattering and gelbstoff absorption is high, as can be seen at station 16 in Figures 7-8. The near-surface maxima of particle scattering and gelbstoff absorption at station 16 coincide with the core of the river plume along the transect, as can be seen in the temperature and salinity data. Near station 16 the gradient of the scattering coefficient is much higher than gradients in the absorption and salinity data. At station 17 high values of particle scattering and chlorophyll extend down to the sea floor, see Figures 8-9. It is assumed but cannot be proved with the available data that this structure is caused by sedimentation of particles through the water column because of a recent presence of the river plume at this position.
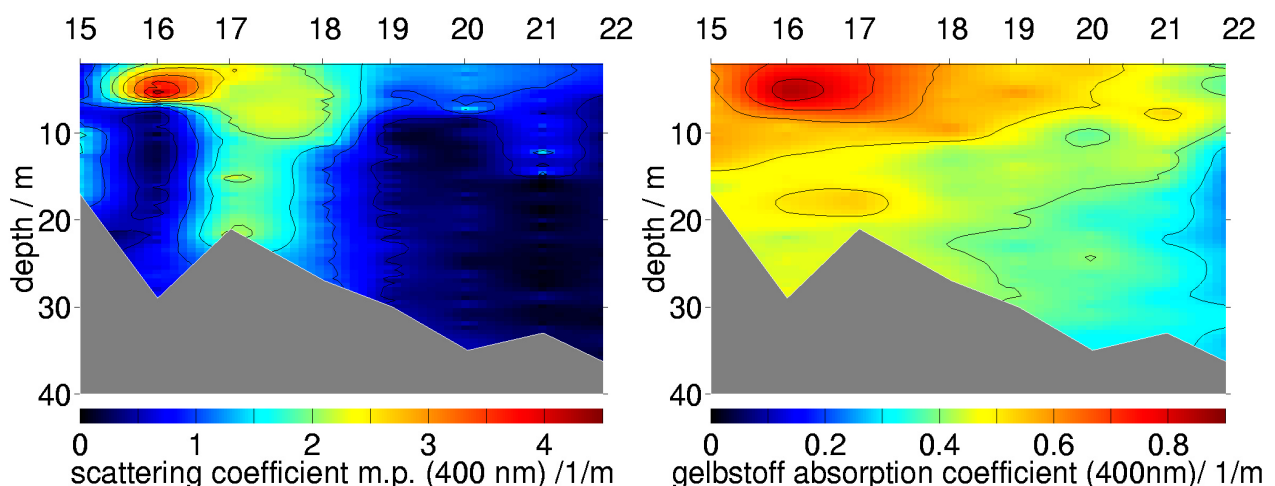
Figures 7 and 8: Isolines of the mineral particle scattering coefficient c_{tp} and the gelbstoff absorption coefficient a_d at 400 nm wavelength in the Seine Bight. Data are calculated from beam attenuation spectra.
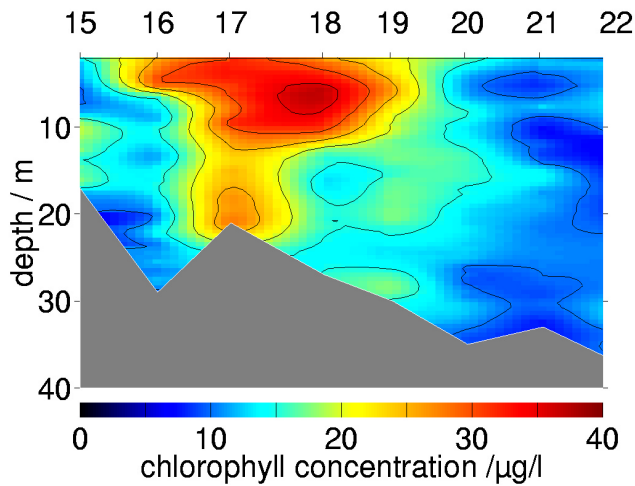
Figure 9: Isolines of chlorophyll in the Seine Bight. Data are calculated from beam attenuation spectra, calibrated with the results of chlorophyll extraction from filtered samples with HPLC.
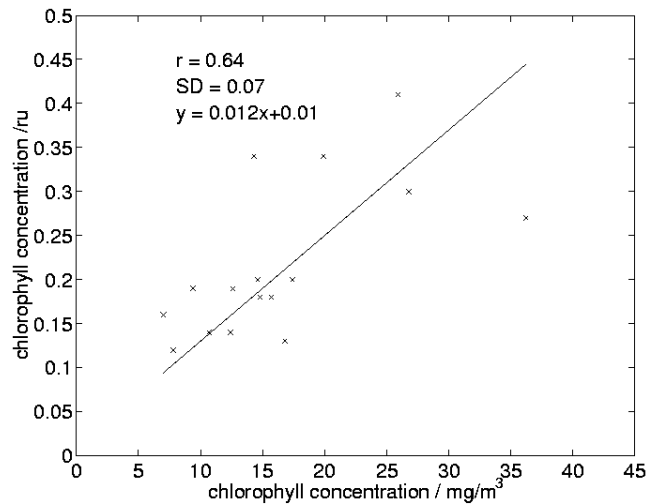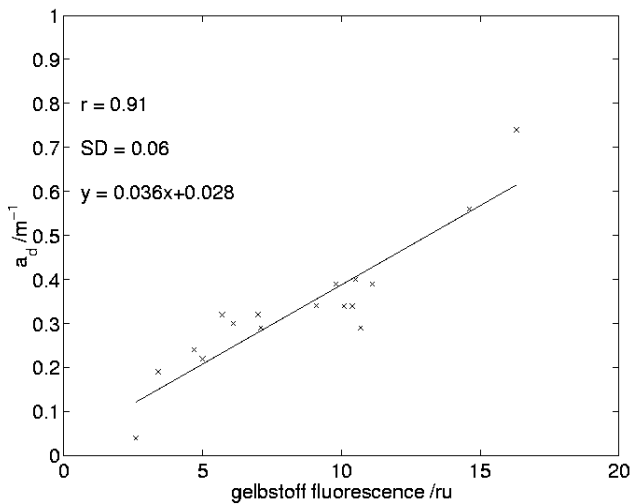
Figures 10 and 11: Comparison of (left) gelbstoff absorption coefficients a_d from transmissometry versus *in situ* fluorescence (270 nm excitation, 420 nm emission, relative units), and (right) chlorophyll data from transmissometry versus chlorophyll a concentrations measured by extraction of filtered samples with HPLC. Correlation coefficients r and standard deviations SD are given in the graphs.
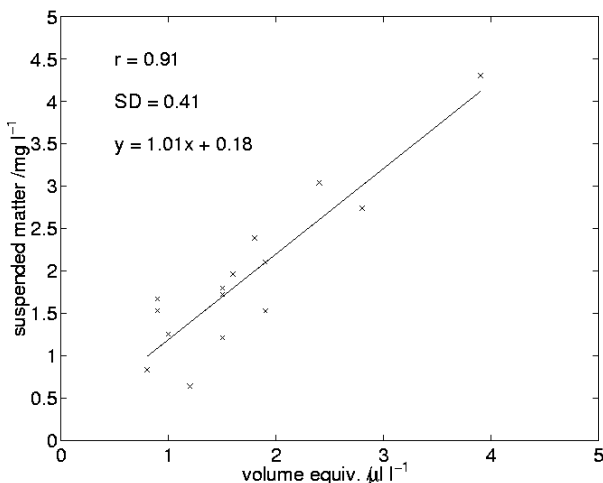
Figure 12: Comparison of volume equivalent (that is, size integrated volume) concentrations of mineral particles in µl/l from transmissometry versus seston (dry weight of suspended particles) derived from filtration using glass fibre filters with 0.45 µm pore size, and weighting of the dry weight.

A test of the reliability of interpreting transmission spectra in terms of substance-specific data is the comparison with data obtained from water samples with standard methods or using other sensors that measure specific data. These correlations are shown in Figures 10-12 for the entire set of data taken along the transect. Taking into account the large range of observed values, the correlation of gelbstoff absorption coefficients versus *in situ* gelbstoff fluorescence and of mineral particles versus suspended matter derived by filtration and weighting is rather good. The correlation of the chlorophyll data is lower but still within the range of uncertainty that is typically found with this biological parameter.

RADIATIVE TRANSFER

For a calculation of a correct light field in case 2 waters it is necessary to take into account the scattering behaviour of the different water constituents. For each class of scattering material a phase function $\tilde{b}$ is calculated. The spectral phase function

$$\tilde{b}(y,l) := \frac{b(y,l)}{b(l)}$$

is defined by normalization of the spectral volume scattering function $b(y,l)$ to the scattering coefficient $b(l)$. Symbol y denotes the scattering angle. For known radii and complex refractive indices of scattering particles and algal cells, the phase function and scattering coefficient can be calculated with Mie theory. As with the attenuation coefficient c, the phase function of all scattering compounds is modelled by a sum of components that are specific to scattering material,

$$\tilde{b}(y,l) = \frac{1}{b(l)} \left(b_{tp}(l)\,\tilde{b}_{tp}(y,l) + b_{pp}(l)\,\tilde{b}_{pp}(y,l) + b_w(l)\,\tilde{b}_w(y,l) \right),$$

with $b = b_{tp} + b_{pp} + b_w$, and the indices tp, pp and w referring to the contributions from transparent (mineral) particles, phytoplankton, and water. Phase function $\tilde{b}_w$ and scattering coefficient b_w of water are taken from the literature.[9] The function $\tilde{b}_{tp}$ is calculated using the particle size distribution parameters from the transmissometer data interpretation, and it holds $b_{tp} = c_{tp}$ with the assumption of transparent particles. The phase function $\tilde{b}_{pp}$ of phytoplankton is calculated with the Mie theory as well, using the particle radius and the complex refractive index estimated from the beam attenuation spectra. The scattering coefficient b_{pp} is assumed to be only weakly affected by absorption, hence $b_{pp} \sim c_{pp}$.

Taking into account these specific contributions due to scattering, a simulation of the light field has been performed for the water column conditions at station 18 of the transect in the Seine Bight. The radiative transfer code uses the matrix operator method[10] for solving the radiative transfer equation. Inelastic sources such as chlorophyll and gelbstoff fluorescence and water Raman scattering are also included in this model. Quantum efficiencies of gelbstoff and chlorophyll fluorescence are taken from the literature,[11,2] and directional isotropy of fluorescence emission is assumed. The water Raman scattering cross section is used,[12] with an anisotropic scattering function $b_w(y,l)$.[13]

Spectra of simulated and measured depth profiles of the scalar irradiance E_0 are given in Figure 12. For simulation, the chlorophyll <u>a</u> concentration is set to 28 µg/l in the upper 15 m of the water column, according to the results of the pigment analysis of water samples. At greater depths, a pigment content of 15 µg/l is estimated from the data shown in Figure 9. The qualitative comparison of both data sets shows a good agreement, Figure 13. The maximum of both spectra is at about 567 nm. The leading and trailing edge of the simulated spectrum at 12.8 m depth shows a significant blue shift of about 10 nm. This might be caused by plankton pigments absorbing at green wavelengths that are not well represented in the modelled spectra, or by the simplified depth profile of chlorophyll used for simulation.
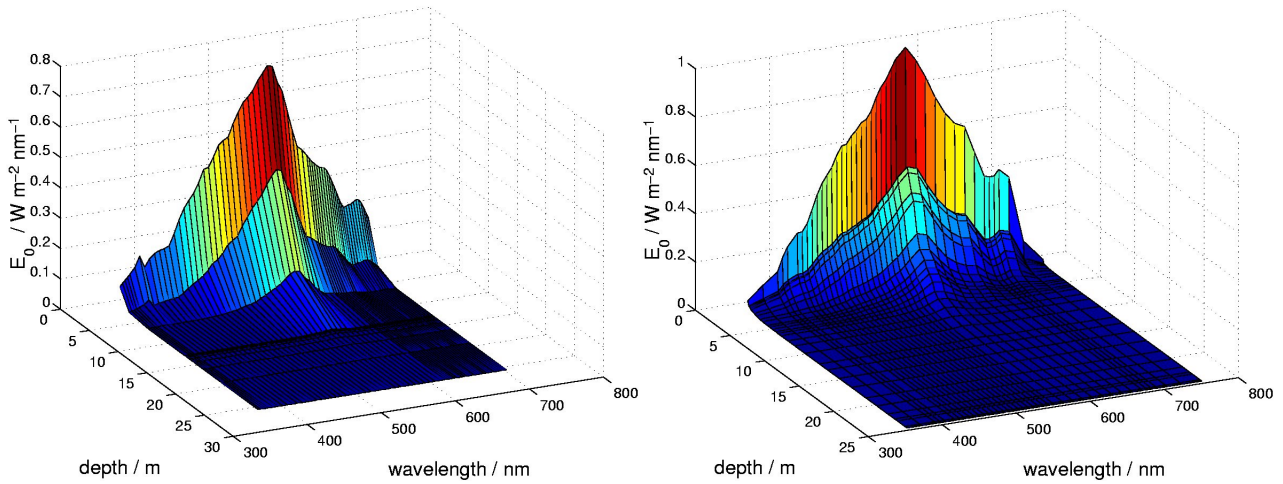
Figure 12. Simulated (left) and measured (right) depth profiles of the scalar irradiance E_O at station 18. Profiling depth is 1.6 to 28 m.
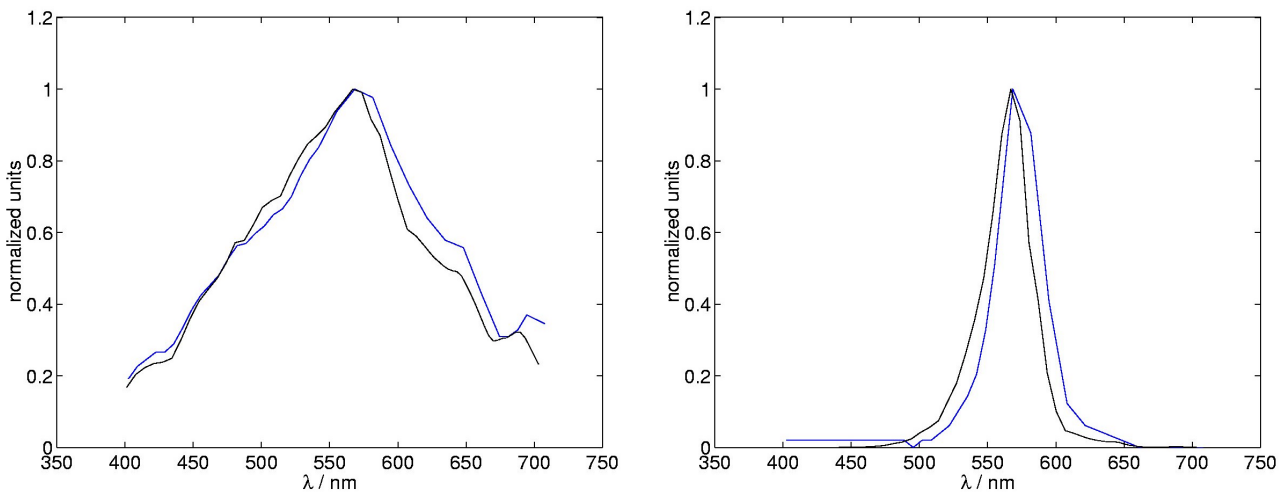
Figure 13. Simulated (black) and measured (blue) spectra of the scalar irradiance E_O at 1.6 (left) and 12.8 m (right) water depth, station 18. The curves are normalized to one at their maximum values at 567 nm.
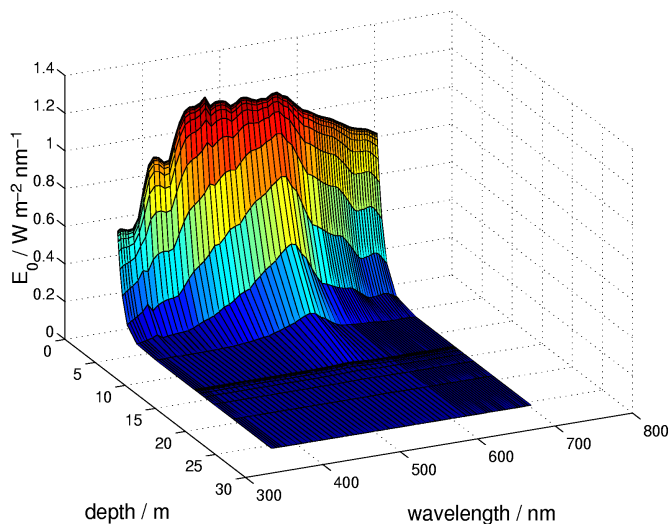
Figure 14. Simulated depth profile of the scalar irradiance E_O at station 18 as shown in Fig 12 (left), but from the sea surface to 28 m depth.

The absolute scalar irradiances differ by up to 0.2 W m^{-2} nm^{-1}. This discrepancy is due to the atmospheric part of the radiative transport model which includes only a few different sets of aerosol attenuation coefficients.[14] This makes it difficult to simulate irradiances at ocean surface level which are identical with those measured with the radiometer. A deck reference sensor for measuring this spectrum was not available. Figure 14 displays this sea surface daylight spectrum and the simulated light field through the entire photic water column.

CONCLUSIONS

Algorithms have been developed which demonstrate the information content of seawater attenuation spectra. They open a way to interpret attenuation coefficients in terms of absorbing and scattering matter, which is of relevance in marine biology and chemistry. Based on this substance-specific information, quantitative data on substance concentrations can be directly derived in cases where such relations exist as, for example, the amount of suspended mineral particles or phytoplankton chlorophyll. In this way, data can be obtained in the form of time series measurements or depth profiles with a time or depth resolution that cannot be achieved with conventional methods such as water sampling and filtration.

Multispectral attenuation coefficients and specific data on absorbing and scattering substances can be used to simulate the underwater light field by solving the radiative transfer equation. Results of these simulations were compared with multispectral data of the irradiance in the water column, showing a good agreement of experimental and modelled data. Hence, the underwater light field can be simulated using information on inherent optical parameters. They are much easier to measure than apparent quantities which depend on daylight, surface waves, and other factors, and are often degraded by ship shadows.

This opens an elegant way to make data available that are relevant for remote sensing using data on inherent optical parameters. For example, the water leaving radiance can be modelled on the basis of depth profiles of attenuation spectra, which is useful for airborne or satellite ocean colour data simulation or validation. The same profiles can also be used for simulations of depth-resolved back-scatter and fluorescence lidar measurements, which is again of high relevance for a validation of depth profiles derived with airborne lidar.

ACKNOWLEDGEMENTS

REFERENCES

1. Kirk, J.T.O. 1983. <u>Light and Photosynthesis in Aquatic Ecosystems.</u> (Cambridge University Press)
2. Mobley, C.D. 1994. <u>Light and Water.</u> (Academic Press)
3. Barth, H., Heuermann, R., Loquay, K. -D, Reuter, R., and Stute, U. 1997. Long-term Stable Sensors For Bio-Optical Measurements. <u>Operational Oceanography. The Challenge for European Co-Operation</u>, edited by Steel, J.H., Behrens, H.W.A., Borst, J.C., Droppert, L.J. and van der Meulen, J.P (Elsevier Oceanography Series, 62, Amsterdam), 133-140.

4. Heuermann, R., Loquay, K.-D. and Reuter, R.. 1995. A multi-wavelength in situ fluorometer for hydrographic measurements. EARSeL Advances in Remote Sensing 3(3):71-77.
5. Højerslev, N.K. 1975. A spectral light absorption meter for measurements in the sea. Limnol. Oceanogr., 20(6): 1024-1034.
6. Barth, H., Grisard, K., Holtsch, K., Reuter, R. and Stute, U. 1997. A polychromatic transmissometer for in situ measurements of suspended particles and gelbstoff in water. Applied Optics, 36:7919-7928.
7. The Practical Salinity Scale 1978 and the International Equation of State of Seawater 1980. Tenth Report on the Joint Panel on Oceanographic Tables and Standards. UNESCO Technical Paper in Marine Science 36, UNESCO, Paris, 1981
8. Press, W.H., Teukolsky, S.A., Vetterling, W.T. and Flannery, B.P. 1992. Numerical Recipes in Fortran (Cambridge University Press)
9. Morel, A. 1974. Optical properties of pure water and pure seawater. Optical Aspects of Oceanography, edited by Jerlov, N.G. and Nielsen, E.S. (Academic Press, London)
10. Plass, G.N., Kattawar, G.W. and Catchings, F.E. 1973. Matrix operator theory of radiative transfer. 1: Rayleigh scattering. Applied Optics, 12(2): 314-329.
11. Haltrin, V.I. and Kattawar, G.W. 1993. Self-consistent solution to the equation of transfer with elastic and inelastic scattering in ocean optics. 1: Model. Applied Optics, 32(27): 5357-5367.
12. Marshall, B.R. and Smith, R.C. 1990. Raman scattering and in-water ocean properties. Applied Optics, 29(1): 71-84.
13. Porto, S.P.S. 1966. Angular dependence and depolarization ratio of the Raman effect. The Optical Society of America, 56(11): 1585-1589.
14. Bartsch, B., Braeske, T., Reuter, R. 1993. Radiative transfer in the atmosphere at operating altitudes of 100 m to 100 km. Applied Optics, 32(33): 6732-6741.